

Review

Do Bioreactor Designs with More Efficient Oxygen Supply to Ovarian Cortical Tissue Fragments Enhance Follicle Viability and Growth In Vitro?

Gerardo Catapano ^{1,*}, Gionata Fragomeni ², Giuseppe Falvo D'Urso Labate ¹,
Luigi De Napoli ¹, Vincenza Barbato ³, Maddalena Di Nardo ³, Valentina Costanzo ³,
Teresa Capriglione ³, Roberto Gualtieri ³ and Riccardo Talevi ³

¹ Department of Mechanical, Energy and Management Engineering, University of Calabria, 87030 Rende (CS), Italy

² Department of Medical and Surgical Sciences, Magna Graecia University, 88100 Catanzaro, Italy

³ Department of Biology, University of Naples Federico II, 80100 Naples, Italy

* Correspondence: gerardo.catapano@unical.it; Tel.: +39-0984-496666

Received: 17 June 2019; Accepted: 10 July 2019; Published: 15 July 2019



Abstract: Background: Autotransplantation of cryopreserved ovarian tissue is currently the main option to preserve fertility for cancer patients. To avoid cancer cell reintroduction at transplantation, a multi-step culture system has been proposed to obtain fully competent oocytes for in vitro fertilization. Current in vitro systems are limited by the low number and health of secondary follicles produced during the first step culture of ovarian tissue fragments. To overcome such limitations, bioreactor designs have been proposed to enhance oxygen supply to the tissue, with inconsistent results. This retrospective study investigates, on theoretical grounds, whether the lack of a rational design of the proposed bioreactors prevented the full exploitation of follicle growth potential. Methods: Models describing oxygen transport in bioreactors and tissue were developed and used to predict oxygen availability inside ovarian tissue in the pertinent literature. Results: The proposed theoretical analysis suggests that a successful outcome is associated with enhanced oxygen availability in the cultured tissue in the considered bioreactor designs. This suggests that a rational approach to bioreactor design for ovarian tissue culture in vitro may help exploit tissue potential to support follicle growth.

Keywords: bioreactor; design; in vitro culture; ovarian tissue; oxygen; transport

1. Introduction

Ovarian tissue cryopreservation and autotransplantation is currently the only option to preserve the fertility of pre-pubertal girls or patients in need of immediate cancer therapy. To date, autotransplantation of frozen/thawed ovarian cortical tissue has yielded about 130 live births worldwide [1]. Clinical application of this procedure is limited by the possible transmission of cancerous cells on the re-implantation of tissue from patients with blood-borne or highly metastatic malignancies [2–4]. The fact that the follicular basal lamina hinders cancerous cell invasion of ovarian follicles [5] has favored the development of two safer alternative strategies. The first strategy is based on the direct isolation and transplantation of isolated primordial follicles [6,7]. The second consists of a multi-step approach to human ovarian tissue culture [8,9] based on: (1) the in vitro culture of ovarian cortical tissue to activate the pool of primordial follicles and promote their growth to the secondary stage, (2) the isolation of secondary follicles from the ovarian stroma, (3) the in vitro culture of isolated follicles to promote the development of antral follicles, and (4) the final aspiration and maturation of cumulus-oocyte-complexes for the in vitro fertilization. Neither of these has yet made it to routine clinical practice. In fact, the isolation of

human primordial follicles is limited by the damage caused by the enzymatic digestion or mechanical disruption of the tough ovarian stromal cortex [10]. Current *in vitro* systems do not provide efficient support to the culture of viable and functional frozen/thawed ovarian tissue and promote the growth of only a limited number of secondary follicles.

Within this framework, considerable research efforts have been undertaken to optimize the culture media and the follicle encapsulating materials used *in vitro* with the intent of bringing the latter approach to the clinic. Reviewing the outcome of such research is beyond the scope of this paper. Detailed information may be found in the excellent reviews [5,11,12] and consensus papers [13] available in the literature.

Less attention has been devoted to the bioreactors used. The bioreactor most widely used for the culture of fragments of fresh or cryopreserved ovarian cortical tissue is still the conventional static culture dish (CD). In CDs, tissue fragments are cultured under a static layer of medium (at times with an oil overlay) under a controlled gaseous atmosphere containing oxygen (O₂) and carbon dioxide (CO₂). Various bioreactor designs have been explored to overcome the limitations associated with the use of CDs [14], which were intended to enhance the transport of dissolved gases (i.e., O₂ and CO₂) from the gaseous atmosphere in the incubator to the follicles in the tissue. The inconsistent results reported [15–19] cast doubt on the fact that the bioreactor designs that enhance gas transport may significantly influence follicle viability and growth in the *in vitro* culture of ovarian cortical tissue. The assumption of this study is that the lack of a rationale in the design of the proposed bioreactors (i.e., the definition of their configuration, geometry, and operation) has thus far prevented exploitation of these bioreactors' performance potential.

To test such an assumption, in this paper a theoretical analysis is proposed of O₂ transport to fragments of ovarian cortical tissue in some exemplary bioreactor designs investigated as an alternative to CDs. The analysis is used to review and seek for a rationale regarding the reported experimental results of an *in vitro* culture of human ovarian cortex fragments. Albeit in an approximate fashion, the theoretical analysis describes the complex interplay between the physical transport of O₂, in the bioreactor and inside the tissue stroma, and its metabolic consumption inside the tissue fragment. Attention was focused on O₂ for a number of reasons. O₂ is important because ovaries have a high oxygen consumption rate per unit of tissue mass (i.e., 1.4 mL/(min 100g_{tissue})) [20] lower only than heart (i.e., 10.7 mL/(min 100g_{tissue})), kidney and liver (i.e., ca. 5 mL/(min 100g_{tissue})), and brain (i.e., 3.5 mL/(min 100g_{tissue})) tissue [21,22]. *In vivo*, during normal growth, the outer layers of the follicle (e.g., the theca layers) are vascularized, which ensures adequate oocyte oxygenation. Poor oxygenation has been associated with cytoplasmic and nuclear abnormalities [23]. *Ex vivo*, grafting of bovine cortical fragments beneath the chorioallantoic membrane of gonadectomized chick embryos has shown that the strip vascularization (and the consequent enhancement of O₂ transport) allowed for the activation of primordial follicles and progression to the secondary stage [24]. *In vitro*, the dissolved O₂ concentration has been reported to affect the development of human embryos [25] and follicles, both in cortical strips [26] and isolated [27–29], as well as the viability of oocytes [30,31], sometimes with inconsistent species-dependent indications. In the *in vitro* culture of fragments of human ovarian cortical tissue, it has been reported that gaseous O₂ concentrations higher than in air ensure adequate oxygenation and promote follicle viability long-term, as well as follicle activation and progression [32]. Recently, it has been shown that too low or too high dissolved O₂ concentrations in tissue are detrimental to both follicle viability and development [19]. In this analysis, the effect of gaseous CO₂ transport was not considered because in Talevi et al. [19], it was shown to be less relevant than O₂, at least for the bioreactors and the conditions investigated therein.

The proposed theoretical analysis associates the culture outcome with oxygen availability in tissue and provides a rationale for the understanding of both the successful and unsuccessful outcome of *in vitro* culture experiments with the considered bioreactor designs. This suggests that a rational approach to the development of novel bioreactors, ensuring that ovarian cells are cultured *in vitro*

under controlled dissolved O_2 concentrations in fragments of human ovarian cortical tissue, might have a significant impact on the exploitation of the full fertility potential of such tissue.

2. Materials and Methods

2.1. Bioreactor Designs

In this review and the analysis herein reported, only papers were included which reported on bioreactor designs with an O_2 supply to follicles in human ovarian cortical tissue that were intended to be more efficient than CDs, where the information reported permitted the estimation of dissolved O_2 transport and metabolic parameters, as well as the comparison of the experimental outcome with CDs.

Information on the considered bioreactor designs is reported in Figure 1 and Table 1. In the conventional dish, taken as the control, O_2 is transported from the above gaseous atmosphere to the upper surface of the tissue fragments across a static layer of medium (Figure 1a). To reach follicles and stromal cells inside the avascular cortex fragment, O_2 has to: (i) partition between the gas and the medium at the gas–medium interface; (ii) be transported across the layer of medium between the gas phase and the upper fragment surface; and (iii) be transported across the fragment thickness, mainly by passive diffusion, while it is consumed by follicular and stromal cells [14]. The poor solubility of O_2 in medium, the resistance to O_2 transport of medium and stromal tissue, and the O_2 metabolic consumption of stromal and follicular cells all contribute to making the dissolved O_2 concentration inside the fragments much lower than in air.

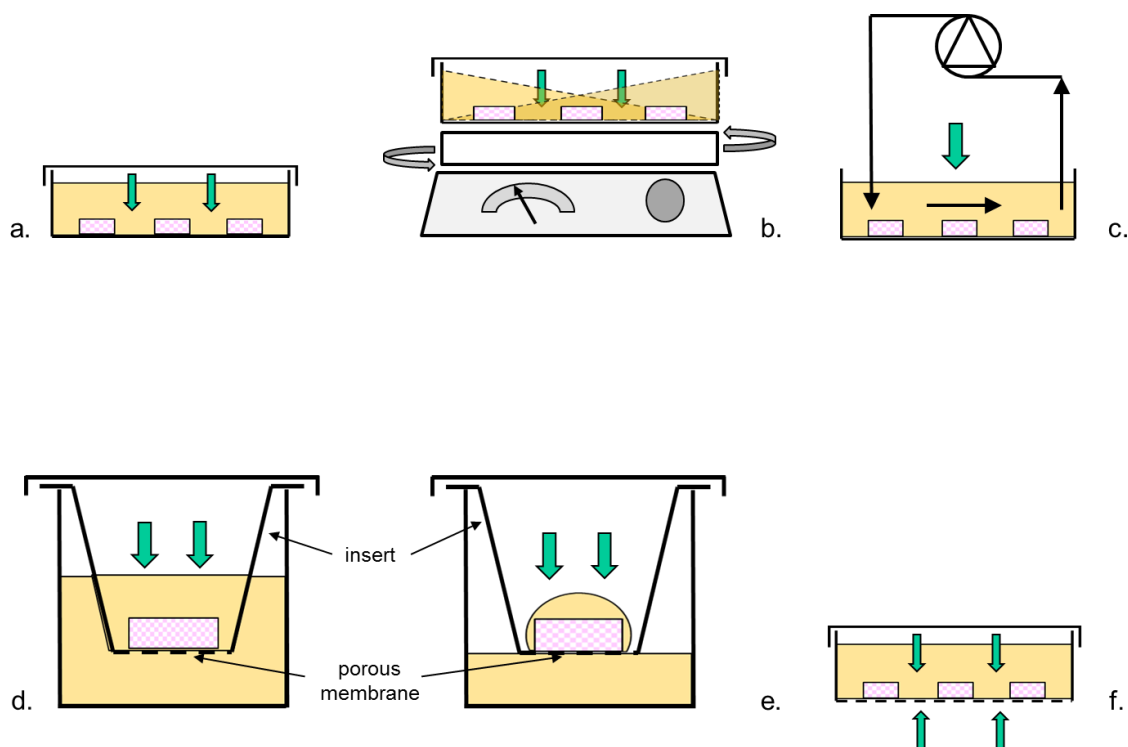


Figure 1. Schemes of the bioreactor configurations used for the *in vitro* culture of fragments of ovarian cortical tissue in the literature reports analyzed in this study: (a) conventional dish (CD), (b) CD with medium mixed by holding the CD on an orbital shaker during culturing [17], (c) CD with medium mixed by recirculating medium above the tissue fragments with an external pump [18], (d) submerged fragment culture on a permeable membrane at the bottom of an insert suspended in a well of a 24-well plate [15,16,33], (e) fragment culture on a permeable membrane at the bottom of an insert suspended in a well of a 24-well plate under a drop of medium [16], and (f) dish with a gas-permeable bottom (PD) [19]. Gas supply portrayed as green arrows.

Table 1. Culture conditions in the literature reports analyzed in this study. Legend for supplements: AA—ascorbic acid; Am—amphotericin; BrG—8-bromo-guanosine; BSA—bovine serum albumin; EGF—epidermal growth factor; FCS—fetal calf serum; FSH—follicle stimulating hormone; Glu—glutamine; ITS—insulin-transferrin-selenium; IHS—inactivated human serum; Ins—insulin; LH—luteinizing hormone; PS—Pen-Strep; Pyr—pyruvate. Abbreviations: Morph—morphological; N—no; Y—yes.

Authors	Medium Used	Growth-Affecting Supplements	Culture System	Support Coating	Culture Mode	No Strips Per Well	Medium Volume	Medium Change	pO ₂	Tissue	Assessment Follicles State						Reference
											Data on Fresh Tissue Y/N	Culture Time Days	Viability	Stage	Grade	Hormones	
Hovatta et al., 1997	-MEM, Earle's	FSH, IHS, Ins, LH, Pyr	Inserts in well in 24 well plate	none, Matrigel™	static, double medium layer	1–3	NA	2nd day	air	Fresh & thawed	Y	up to 21	Morph	Y	N	N	[15]
Wright et al., 1999	-MEM,	FSH, HSA, ITS-G BrG, cMP	Inserts in well in 24 well plate	Matrigel™	static, double medium layer	NA	100 uL + 400 uL	150 uL @ 2nd day	air	Fresh	Y	up to 14	Morph	Y	N	N	[16]
Isachenko et al., 2006	Iskove's modified Dulbecco's	EGE, FCS, FSH, ITS,	200 mL dishes	none	static vs. mixed on orbital shaker	20	30 mL	NO	air	Fresh & thawed	N	up to 21	Morph	Y	N	N	[17]
Liebenthron et al., 2013	McCoy's 5a + HEPES	AA, BSA, Glu, ITS	6 well plate	none	static vs. medium recirculation	NA	4.5 mL	NO	air	Fresh	Y	up to 6	Morph calcein AM	Y	N	Y	[18]
Talevi et al., 2018	-MEM	AA, Am, BSA, Glu, ITS, PS	50 mm dishes	none	static, conventional vs. permeable bottom	10	5 mL	half every other day	air	Fresh	Y	up to 9	Morph dead/live	Y	Y	N	[19]

To enhance the O_2 transport from the gas/medium interface to the upper fragment surface, it has been proposed that the medium be mixed either by holding CDs on an orbital shaker (Figure 1b) [17], or by periodically recirculating medium above the fragments with an external pump (Figure 1c) [18] during culturing. Alternatively, it has been that the O_2 be supplied from both the upper and the lower surface of the tissue fragments. This has been pursued either by culturing the fragments on permeable inserts suspended in a well of a multi-well plate submerged in static medium (Figure 1d–e) [15,16], or in dishes with a gas-permeable bottom (PD) (Figure 1f) [19]. In both cases, minimization of the resistance to O_2 transport external to the fragments has been pursued using a culture under medium layers of decreasing thicknesses. In a few cases, O_2 transport to follicles has been enhanced by decreasing the thickness of the tissue fragments [15,33].

2.2. Models of Oxygen Transport

To investigate possible associations between culture outcome and the level of oxygen at which ovarian cells are cultured inside a fragment, estimates of the dissolved oxygen concentration anywhere in the tissue fragment are needed for varying bioreactor designs and operating conditions. In this analysis, such estimates were obtained by developing mathematical models describing the transport of dissolved oxygen from the gaseous oxygen source across the medium and inside the ovarian cortical tissue for the bioreactors and the operating conditions used for the considered papers. In the transport models, the considered bioreactors were schematically described, as shown in Figure 2. The tissue fragments were approximated as a single tissue slab, entirely covering the bottom of the dish or the insert, with uniform transport and metabolic properties. The latter assumption implies that follicles are uniformly distributed in the tissue, are all at the same developmental stage, and consume O_2 at the same rate. O_2 was assumed to be supplied only through the upper (in some cases also the lower) fragment surface at a steady rate. According to the film theory [34], the resistance to O_2 transport at any interface between the medium and tissue is concentrated in a stagnant layer of medium adherent to the tissue surface, the thickness of which depends on the bioreactor geometry, the volume of medium used, and the degree of medium mixing. In statically operated bioreactors, the stagnant layer thickness equals the height of medium under which tissue is cultured. In bioreactors in which the medium is mechanically or fluid-mechanically mixed, the resistance to O_2 transport was estimated in terms of an O_2 transport coefficient, k_L , from available semi-empirical correlations for the given bioreactor geometry and fluid dynamic conditions. The model assumes that an anoxic zone forms farthest from the O_2 source if O_2 is supplied only from the upper fragment surface, or in the middle of the fragment thickness if O_2 is supplied from both the upper and the lower fragment surfaces.

The O_2 transport model for each bioreactor design was based on previously published models for dissolved O_2 transport in ovarian cortical tissue cultured under a layer of stagnant medium in CDs and PDs [19]. For this reason, each model's description may resemble, occasionally verbatim, that reported in Talevi et al. [19]. Briefly, in bioreactors in which O_2 is supplied only through the upper fragment surface (Figure 2a), the mass balance equations for O_2 in tissue were obtained in analogy to purely diffusive heat transport in a homogeneous slab when the resistance to transport from the liquid in contact with the slab to the slab outer surface is not negligible [34]. A reference system was used with a z -axis with the origin at the lower fragment surface, oriented towards the medium above. The mass balance equations were expressed in dimensionless form to minimize the bias caused by the lack of reliable estimates of the geometric, transport, and metabolic properties of the ovarian cortical tissue fragments. This also suggests how such properties combine in the dimensionless groups to determine the dissolved O_2 concentration profile across the tissue fragment (and the bioreactor performance). The dimensionless dissolved O_2 concentration in tissue, C_T^* , and the dimensionless space coordinate, z^* , were defined with respect to the dissolved O_2 concentration that equilibrates with the gaseous O_2 pressure at the gas-medium interface, C_B , and the fragment thickness, δ_T , respectively, as follows:

$C_T^* = C_T/C_B$ and $z^* = z/\delta_T$. The one-dimensional steady state mass balance of O_2 about an infinitesimal tissue control volume Adz yields:

$$\frac{d^2 C_T^*}{dz^{*2}} = \frac{G'''}{D_T C_B} \delta_T^2 = \phi^2 \quad (1)$$

subject to the following boundary conditions:

$$\text{BC1: } z^* = 1 \left. \frac{d C_T^*}{dz^*} \right|_{z^*=1} = \frac{k_L}{D_T} \delta_T (1 - C_T^*(z^* = 1)) = Bi_m (1 - C_T^*(z^* = 1)) \quad (2a)$$

$$\text{BC2: } z^* = \delta_{i,U}/\delta_T \quad C_T^* = 0 \quad (2b)$$

where $\delta_{i,U}$ is the distance from the fragment bottom at which the anoxic zone begins. BC1 states that the oxygen transported across the medium diffuses into the tissue at the same rate.

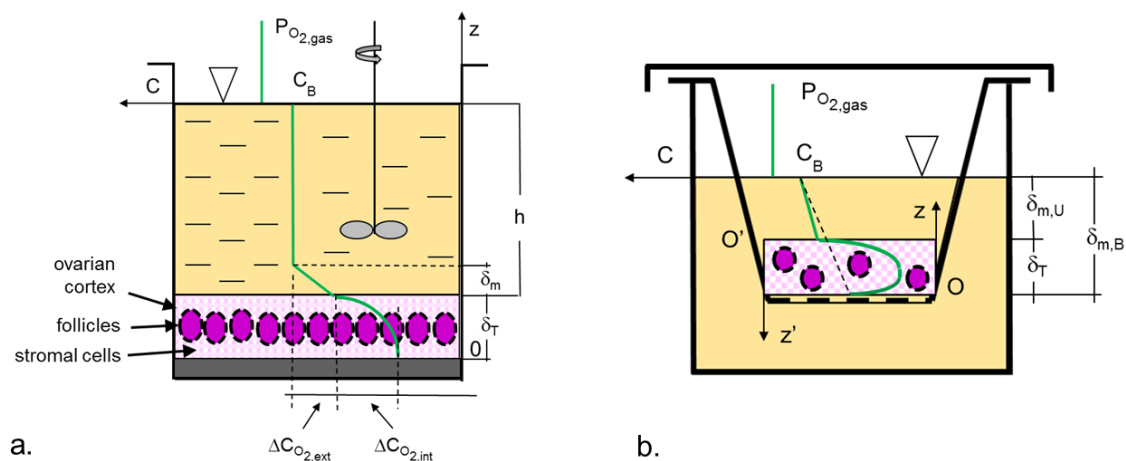


Figure 2. Bioreactor schemes used for the transport models and qualitative dissolved oxygen concentration profile in the medium and inside the fragment: (a) conventional or mixed dish in which oxygen is supplied only through the upper fragment surface, and (b) submerged fragment culture on a permeable membrane at the bottom of an insert suspended in a well of a 24-well plate. Captions: C —dissolved oxygen concentration; C_B —dissolved oxygen concentration in the medium at equilibrium with $pO_{2,gas}$; $pO_{2,gas}$ —gaseous oxygen tension above the medium surface; δ_m and $\delta_{m,U}$ or $\delta_{m,B}$ —thickness of the medium layer above or below the strip, respectively; δ_T —thickness of the tissue fragment; $\Delta C_{O_2,ext}$ —external dissolved oxygen concentration drop in the medium; $\Delta C_{O_2,int}$ —internal dissolved oxygen concentration drop in the fragment. Other symbols are defined in the text. Please note that drawings are not to scale.

Integration of Equations (1) and (2) yields the dimensionless dissolved O_2 concentration C_T^* at any dimensionless distance z^* from the bottom of the fragment, as follows [19]:

$$C_T^* = \frac{1}{2} \phi^2 \left[\left(\frac{\delta_{i,U}}{\delta_T} \right)^2 + \left(\frac{z}{\delta_T} \right)^2 - 2 \frac{\delta_{i,U}}{\delta_T} \frac{z}{\delta_T} \right] \quad (3)$$

with

$$\frac{\delta_{i,U}}{\delta_T} = 1 - \left[\frac{1}{\phi} \sqrt{\frac{\phi^2}{Bi_m^2} + 2} - \frac{1}{Bi_m} \right]; \quad \phi^2 = \frac{G'''}{D_T C_B} \delta_T^2; \quad Bi_m = k_L \frac{\delta_T}{D_T} \quad (4)$$

where: D_m and D_T are the O_2 diffusivity in the medium and tissue, respectively; G''' is the cellular O_2 consumption rate per unit tissue volume; δ_m and δ_T is the thickness of the stagnant medium layer above the fragment and the fragment thickness, respectively; Bi_m is the dimensionless mass Biot number at

the upper fragment surface; and ϕ is the dimensionless Thiele modulus. ϕ compares the maximal rate of O_2 cellular consumption to its diffusion in tissue. Bi_m compares the dissolved O_2 concentration drop inside the tissue to that in the stagnant medium layer adhering on the given fragment surface through which O_2 is supplied to the ovarian cells in the fragment.

In bioreactor designs in which O_2 is also supplied through the lower fragment surface (Figure 2b), the formation of an anoxic zone in the middle of the fragment permits us to obtain the dissolved O_2 concentration profile in the lower part of the fragment independent of the O_2 supply from the upper surface. The mass balance equations for the dissolved O_2 concentration in the lower part of the tissue fragment were written with reference to a z' -axis with origin O' at the upper fragment surface and oriented towards the medium below. In bioreactor designs in which O_2 is transported across a layer of stagnant medium in contact with the lower fragment surface, the boundary conditions were assumed to be identical to Equation (2), but for the Bi_m at the lower fragment surface. Integration of the mass balance equations and boundary conditions yields the dissolved O_2 concentration profiles and the distance at which the anoxic zone begins to form from the bottom, $\delta_{i,B}$, similar to Equations (3) and (4). The transformation $z' = \delta_T - z$ yields the actual profiles in terms of z and z^* . In bioreactors in which the tissue fragment is in direct contact with a gas-permeable membrane exposed to the same gaseous atmosphere as the medium above the tissue, Equation (2a) was replaced by the condition stating that the dissolved O_2 concentration at the lower tissue surface equals C_B . The integration of the mass balance equation and the new boundary conditions yields [19]:

$$C_T^* = \left[1 + \frac{1}{2} \phi^2 \left(\frac{z}{\delta_T} \right)^2 - \sqrt{2} \phi \left(\frac{z}{\delta_T} \right) \right] \quad (3')$$

Equations (3), (4), and (3') show that the dissolved O_2 concentration in tissue depends on the O_2 transport properties in medium and tissue, on the cellular O_2 metabolic consumption, and on the fragment geometry, as well as on the bioreactor geometry and fluid dynamics described by the dimensionless Thiele modulus, ϕ , and the mass Biot number, Bi_m . Model predictions were obtained for $C_B = 0.2 \text{ mol/m}^3$ (corresponding to a $pCO_{2,gas}$ of about 21%), $D_T = 2.8 \times 10^{-9} \text{ m}^2/\text{s}$, $D_m = 3.5 \times 10^{-9} \text{ m}^2/\text{s}$, $G''' = 2 \times 10^{-2} \text{ mol}/(\text{s}\cdot\text{m}^3)$ [19], assuming a density $\rho = 9.97 \times 10^2 \text{ kg/m}^3$ [35] and a dynamic viscosity $\mu = 8.2 \times 10^{-4} \text{ kg}/(\text{m}\cdot\text{s})$ for the medium [36].

The efficiency of O_2 transport to the tissue was expressed in terms of the oxygen availability in the tissue (i.e., the volume-averaged dissolved O_2 concentration in the fragment), $C_{T,avg}$, and the width of the anoxic zone, w_{az} . w_{az} was defined as $w_{az} = \delta_{i,U}$ in bioreactors in which O_2 is supplied only through the upper fragment surface, and as $w_{az} = \delta_{i,U} - (\delta_T - \delta_{i,B})$ in bioreactor designs in which the O_2 is supplied through both fragment surfaces.

2.3. Estimation of the Oxygen Transport Coefficient, k_L

2.3.1. Static Bioreactors

In static bioreactors, O_2 is transported by pure diffusion across the layer of stagnant medium between the gas-medium interface and the fragment surface. Hence, k_L was estimated as the ratio of the O_2 diffusivity in the medium to the stagnant medium layer thickness, $k_L = D_m/\delta_m$. In bioreactors in which O_2 is supplied only across the upper fragment surface, δ_m was estimated using the medium volume used for the culture for a dish diameter of 14.5 cm [17] or 3.5 cm [18]. In the bioreactors used for the culture on an insert, and in which O_2 is supplied across both the upper and the lower fragment surface, the diameter of a well in a 24-well plate was assumed to be equal to 1.56 cm [15,16,33]. The thickness of the upper medium layer, $\delta_{m,U}$, was estimated from the medium volume by neglecting both the insert and membrane volumes and by assuming a 1 mm distance between the bottom of the insert and the well [15,33,36,37] or it was assumed to be equal to 500 μm (as for experiment III in Wright et al. [16]). The thickness of the lower medium layer, $\delta_{m,B}$, was estimated from the medium

volume assuming a straight diffusive path for O₂ from the gaseous phase to the membrane bottom in the insert, as shown in Figure 2b.

2.3.2. Mixed Bioreactors

In mixed bioreactors, the O₂ transport coefficient in medium, k_L , was estimated using available semi-empirical correlations for the given bioreactor type, geometry, and fluid dynamic conditions. In large dishes held on an orbital shaker [17], the increase of the gas exchanging surface area caused by the shaking may be neglected [38]. Hence, k_L was estimated by adapting the following semi-empirical correlation for shaking flasks to circular dishes [39]:

$$k_L a = 0.5 d^{73/36} n d_o^{1/4} V_m^{-8/9} D_m^{1/2} \nu^{13/54} g^{-7/54} \quad (5)$$

where a is the gas exchanging medium surface-to-volume ratio in the dish, d is the inner dish diameter, d_o is the shaking orbit diameter, n is the shaking frequency, V_m is the medium volume, $\nu = \rho/\mu$ is medium kinematic viscosity, and g is the gravitational acceleration. Model predictions were obtained for an orbital diameter $d_o = 1.9$ cm.

In culture dishes in which the medium is periodically recirculated above the tissue fragments, the actual fluid dynamic depends on the position and geometry of the influent and effluent cannulas. In the absence of such information, transport efficiency was estimated by assuming that the medium continuously flows as a plug above the fragments located at the bottom of the dish. The local k_L value corresponding at any given chord length normal to medium flow in the dish was estimated from the following semi-empirical correlation [40]:

$$k_L z/D_m = 0.323 (v(z)z/\nu)^{1/2} \left(\frac{\nu}{D_m}\right)^{1/3} \quad (6)$$

where z is the distance from the inlet section and $v(z)$ is the current medium velocity at the distance z . A k_L value averaged over the dish surface, $k_{L,avg}$, was used to obtain model predictions.

3. Results and Discussion

Equations (3) and (4) show that in static CDs, the actual dissolved O₂ concentration inside the tissue depends on the gaseous O₂ pressure (i.e., C_B), on the resistance to O₂ transport of the medium layer and tissue (i.e., $1/k_L$ and δ_T/D_T), and on the metabolic rate at which the cells in the ovarian cortex consume O₂ (i.e., G'''). Optimization of bioreactor design to provide ovarian cells with an adequate O₂ supply has often been approached by trying to optimize some of the above variables one at a time (e.g., either C_B , or k_L , or else δ_T) directly in culture experiments. Such an approach has often yielded inconsistent results. For instance, an increase of the O₂ transport coefficient, k_L , obtained either by increasing the degree of medium mixing [17,18] or by decreasing the thickness of the upper medium layer (i.e., between the gaseous atmosphere and the upper fragment surface) [15,16,33] has not always enhanced follicle viability.

Theoretical models of O₂ transport may help in understanding the interplay among contributing variables and parameters and the reported culture outcome. Models have been proposed to describe dissolved O₂ transport in pre-antral and antral follicles [41–44] that account to varying degrees for the changing position and geometry of the oocyte in the growing follicle when the dissolved O₂ concentration outside the follicle equals that in the blood vessels surrounding it. Such models have been valuable for understanding the role of antrum formation and of follicular cells' metabolism in ensuring adequate oxygenation to the oocyte in the preovulatory follicle in vivo. The use of such models to estimate O₂ availability to follicles in fragments of ovarian cortical tissue cultured in vitro is impractical. In fact, they do not account for the effects on O₂ transport from an external gaseous source of the stromal extracellular matrix and the cells in cortical tissue, nor for bioreactor geometry and fluid dynamics.

The models discussed here describe O₂ transport in fragments of ovarian cortical tissue cultured in vitro in various bioreactor designs, and account, albeit in an approximate fashion, for tissue properties and bioreactors geometry and fluid dynamics. Ideally, the models ought to describe the extent to which the different cells and stroma components present in tissue determine its transport and metabolic properties. Bioreactor geometry and fluid dynamics should also be described in detail. The scarcity of reliable quantitative information on the composition and structure of the ovarian cortical tissue, the metabolic functions of the ovarian cells, and the bioreactors used makes it challenging to build reliable complex transport models. To obtain qualitative predictions of the dissolved O₂ distribution inside a tissue fragment, a less detailed but effective description of ovarian cortical tissue was used in terms of uniform lumped transport and metabolic characteristics, the value of which could be estimated from literature information for human ovarian cortex or similar tissue. Results and model predictions obtained for different bioreactor designs were generally compared when reported in the same paper, or in different papers by the same research group, to minimize the bias caused by the broad variability of medium composition and supplements, and of the methods used to assess follicle viability and stage. The broad variability of the follicle number and stage in ovarian cortical tissue from different species and age, and even in tissue harvested from different regions of the same ovary [45], contributes to making data interpretation even more problematic.

The model-predicted O₂ availability and width of the anoxic zone inside the tissue fragment for the considered bioreactor configurations and operating conditions are reported in Table 2. The value of ϕ , consistently greater than unity, suggests that, under all conditions, the dissolved O₂ concentration in tissue steeply decreases towards the innermost regions of the fragment as a result of the large diffusional resistance of tissue, the more so the greater the ϕ [46]. The value of Bi_m varies by two orders of magnitude and suggests that the interplay of transport and metabolic phenomena is rather different in the various bioreactor configurations yielding broadly different dissolved O₂ concentrations at the tissue–medium interfaces. In bioreactors in which O₂ is supplied only from the upper fragment surface, Equations (3) and (4) suggest that the combination of ϕ and Bi_m , rather than each single group, determines the dissolved O₂ concentration profile inside tissue and the width of the anoxic zone, w_{az} . In bioreactors in which O₂ is also supplied through the lower fragment surface, the dissolved O₂ profile inside tissue and w_{az} is determined by the combination of the values of ϕ and Bi_m at both medium-fragment interfaces.

First, the models were used to analyze the inconsistent results obtained with bioreactors in which O₂ transport is enhanced with respect to CDs by increasing k_L (bioreactor #3 vs. #4 and bioreactor #5 vs. #6 in Table 2). The transport models predicted a very poor O₂ availability and an anoxic zone well in excess of 95% of the fragment thickness when the fragments are cultured on an insert in a well, both under an upper medium layer about 2.3 mm thick and a much thinner layer of about 0.5 mm (i.e., bioreactors #5 vs. #6 in Table 2) [16]. Similar predictions were obtained for fragments cultured in static CDs or in CDs in which the medium was mixed by recirculating it above the fragments with an external pump (i.e., bioreactor #3 vs. #4 in Table 2) [18]. The models' predictions suggest that the bioreactor designs used did not ensure a good O₂ supply to the ovarian cells, irrespective of how they were operated. Under such conditions, cells likely starved for O₂ and struggled for survival. It is no surprise that follicle viability was not found to be any different between each pair of bioreactors.

Second, the models were used to analyze the successful results obtained with bioreactors in which O₂ transport is enhanced by increasing k_L or by decreasing the fragment thickness, δ_T . In bioreactors in which k_L is enhanced with respect to static CDs by holding the CDs on an orbital shaker during culture [17] (i.e., bioreactors #1 vs. #2 in Table 2), the models predicted a much higher O₂ availability and an anoxic zone about 20% smaller in mixed CDs than in static CDs (Table 2). Correspondingly, the number of viable follicles was about 2.6 times higher, with a higher proportion of morphologically intact follicles, than in CDs. Also, in bioreactors in which tissue fragments were statically cultured under a layer of medium at the bottom of gas permeable dishes (PDs), in direct contact with an O₂ source [19] (i.e., bioreactor #8 vs. #9 in Table 2) the models predicted a higher O₂ availability in PDs

than in CDs with a gas-impermeable bottom. Correspondingly, the width of the anoxic core in PDs was one third of that in CDs. Histological and viability analysis showed that culture in PDs for up to 9 days enhanced the follicle viability and progression to the secondary stage over cultures in CDs. In one case, the tissue resistance to oxygen transport was reduced by culturing tissue fragments of decreasing thickness (i.e., 2 vs. 0.3 mm) on an insert placed in a well of a 24-well plate (i.e., bioreactors #5 vs. #7 in Table 2) [15,16]. The models predicted an O₂ availability two times higher and a 15% smaller anoxic zone in the bioreactors with thinner tissue fragments. Correspondingly, the number of atretic follicles in thinner fragments was about one fourth of that in thicker fragments (4% vs. 17%, respectively).

That which is reported above shows that models of O₂ transport in the ovarian cortex and bioreactors provide rational grounds for understanding the experimental results reported for all considered bioreactors, some of which would otherwise appear inconsistent. This lends support to this study's assumption that the rational optimization of bioreactor design for the *in vitro* culture of fragments of ovarian cortical tissue may ensure adequate oxygenation to the ovarian cells and may enhance follicle viability and growth. A reliable transport model that predicts the dissolved O₂ concentration anywhere in the tissue fragment as a function of its value in the medium bulk for a given fragment and bioreactor geometry and fluid dynamics would also provide a means to indirectly monitor the dissolved O₂ concentration in tissue from measurements of the dissolved O₂ concentration in the medium bulk, the only measurable parameter. This would make it possible for an operator to change the operating conditions and adjust the supply of O₂ (and also of nutrients and metabolic effectors) to the current cell metabolic requirements so as to maintain the follicles viability and possibly guide their progression during culture.

A model, however, is as good as its assumptions and its parameters estimates. To increase the reliability of a model's predictions, it would be necessary to quantitatively characterize the structure of the ovarian cortical tissue and the metabolic requirements of the ovarian cells at any developmental stage. Flow and mass transport in the bioreactor ought to be based on a more detailed description of bioreactor and fragment geometry. CO₂ transport and the effect of pericellular pH changes on ovarian cell metabolism should also be accounted for because they might also play a role in bioreactor configurations with a high tissue-to-medium volume ratio.

In spite of its limitations, the model-based review and analysis of reports on the *in vitro* culture of fragments of ovarian cortical tissue suggests that bioreactor designs enhancing the O₂ supply to the ovarian cells have the potential to maintain about 65% [19] of follicles as viable for longer than a week, and to activate up to about 20% of these [8,15,19] to progress from the primordial to the secondary stage, without significant differences between fresh and frozen-thawed tissue. However, in the long-term, *in vitro* culture follicle quality decreases (with only 45% grade I follicles after 9 days of culture [19], and the proportion of viable follicles decreases as well. Correspondingly, the proportion of degenerating/atretic follicles increases from a few units to 14–50% [8,15] after a week of culture. This suggests that there is still quite some room to further optimize bioreactor design to enhance O₂ transport to ovarian cells and to adjust it to their changing requirements as follicles grow, as a possible means to guide their progression *in vitro*.

Table 2. Model-predicted oxygen availability, CT, avg, width of anoxic zone, w_{ac}, and O₂ concentration at tissue medium interface, CT, m, for the bioreactor geometry and fluid dynamic conditions used in the literature reports analyzed in this study. Other symbols are defined in the text.

Bioreactor #	Bioreactor Type	Fragment Side of O ₂ Supply	δ_T m	δ_m m	k_L m/s	Thiele Number ϕ	Biot Bi_m	Oxygen Availability		Anoxic Core w_{ac}/δ_T %	Reference
								$C_{T,m}/C_B$ %	$C_{T,avg}/C_B$ %		
1	Static CD	Upper	1.00×10^{-3}	8.18×10^{-4}	4.28×10^{-6}	6.0	1.53	3.07	3.07×10^{-3}	95.85	[17]
2	CD on orbital shaker	Upper	1.00×10^{-3}	NA	1.13×10^{-4}	6.0	40.37	81.14	3.15×10^{-1}	78.68	[17]
3	Static CD	Upper	1.00×10^{-3}	3.69×10^{-3}	9.49×10^{-7}	6.0	0.34	0.16	1.60×10^{-4}	99.05	[18]
4	CD w/ periodic medium flow	Upper	1.00×10^{-3}	NA	9.94×10^{-7}	6.0	0.36	0.18	1.76×10^{-4}	99.01	[18]
5	Culture on insert in well	Upper	2.00×10^{-3}	2.26×10^{-3}	1.55×10^{-6}	12.0	1.10	0.42	5.44×10^{-4}	98.82	[16]
		Lower		4.26×10^{-3}	8.21×10^{-7}		0.59	0.12			
6	Culture on insert in well	Upper	2.00×10^{-3}	5.00×10^{-4}	7.00×10^{-6}	12.0	5.00	7.49	1.69×10^{-5}	95.61	[16]
		Lower			2.33×10^{-6}		1.67	0.95			
7	Culture on insert in well	Upper	3.00×10^{-4}	1.33×10^{-3}	2.63×10^{-6}	1.8	0.28	1.20	1.53×10^{-3}	84.25	[15]
		Lower		1.63×10^{-3}	2.15×10^{-6}		0.23	0.81			
8	Static CD	Upper	5.00×10^{-4}	1.40×10^{-3}	2.50×10^{-6}	2.5	0.7	3.6	5.30×10^{-2}	89.3	[19]
9	Static PD	Lower	5.00×10^{-4}	1.40×10^{-3}	2.50×10^{-6}	2.5	0.7	3.6	1.25	32.6	[19]
					NA				100		

4. Conclusions

The critical review reported in this paper was aimed at investigating whether the lack of a rationale to the design of the proposed bioreactor designs for the in vitro culture of fragments of cortical ovarian tissue has prevented the full understanding of the effect of O₂ transport on the culture outcome, and from fully exploiting the tissue fertility potential. Theoretical models were developed for O₂ transport from a gaseous atmosphere to cells in ovarian cortical tissue fragments in some exemplary bioreactors proposed to enhance O₂ transport in in vitro culture. The models were used for predicting the dissolved O₂ concentration anywhere in the fragment. The model-based analysis evidenced an association between higher O₂ availability in tissue and an enhanced follicle viability and progression. It also provided a rationale to help understand the unsuccessful reported culture outcomes. This suggests that bioreactor designs enhancing O₂ transport to cells in fragments of cortical ovarian tissue may significantly influence the outcome of the in vitro culture. It also suggests that future strategies to maintain follicle viability long-term and possibly guide follicle activation and growth are better based on bioreactors for the in vitro culture of ovarian tissue designed and operated according to rational engineering criteria to control the perfollicular culture microenvironment. Within this methodological framework, models describing the transport of medium flow and relevant dissolved species in bioreactors and tissue in detail may be valuable developmental tools, provided that their predictions are validated against experimental measurements.

Author Contributions: Conceptualization—G.C., T.C., R.G., and R.T.; Methodology—G.C., G.F.D.L., and G.F.; Formal analysis—All Authors; Software—G.C., G.F., G.F.D.L., and L.D.N.; Resources—V.B., M.D.N., V.C., R.G., and R.T.; Writing—Original Draft Preparation—G.C., R.G., and R.T.; Writing—Review and Editing—All Authors.

Conflicts of Interest: The authors declare no conflict of interest.

References

1. Donnez, J.; Dolmans, M.M. Fertility preservation in women. *N. Engl. J. Med.* **2018**, *378*, 399–401.
2. Donnez, J.; Silber, S.; Andersen, C.Y.; Demeestere, I.; Piver, P.; Meirow, D. Children born after autotransplantation of cryopreserved ovarian tissue. A review of 13 live births. *Ann. Med.* **2011**, *43*, 437–450. [[CrossRef](#)] [[PubMed](#)]
3. Dolmans, M.M.; Luyckx, V.; Donnez, J.; Andersen, C.Y.; Greve, T. Risk of transferring malignant cells with transplanted frozen-thawed ovarian tissue. *Fert. Steril.* **2013**, *99*, 1514–1522. [[CrossRef](#)] [[PubMed](#)]
4. Abir, R.; Aviram, A.; Feinmesser, M.; Stein, J.; Yaniv, I.; Parnes, D. Ovarian minimal residual disease in chronic myeloid leukaemia. *Reprod Biomed. Online* **2014**, *28*, 255–260. [[CrossRef](#)] [[PubMed](#)]
5. Abir, R.; Nitke, S.; Ben-Haroush, A.; Fisch, B. In vitro maturation of human primordial ovarian follicles: Clinical significance, progress in mammals, and methods for growth evaluation. *Histol. Histopathol.* **2006**, *21*, 887–898.
6. Carroll, J.; Gosden, R.G. Transplantation of frozen-thawed mouse primordial follicles. *Hum. Reprod.* **1993**, *8*, 1163–1167. [[CrossRef](#)] [[PubMed](#)]
7. Kniazeva, E.; Hardy, A.N.; Boukaidi, S.A.; Woodruff, T.K.; Jeruss, J.S.; Shea, L.D. Primordial follicle transplantation within designer biomaterial grafts produce live births in a mouse infertility model. *Sci. Rep.* **2015**. [[CrossRef](#)]
8. Telfer, E.E.; McLaughlin, M.; Ding, T.; Thong, K.J. A two-step serum-free culture system supports development of human oocytes from primordial follicles in the presence of activin. *Hum. Reprod.* **2008**, *23*, 1151–1158. [[CrossRef](#)]
9. McLaughlin, M.; Albertini, D.F.; Wallace, W.H.B.; Anderson, R.A.; Telfer, E.E. Metaphase II oocytes from human unilaminar follicles grown in a multi-step culture system. *Mol. Hum. Reprod.* **2018**, *24*, 135–142. [[CrossRef](#)]
10. Hornick, J.E.; Duncan, F.E.; Shea, L.D.; Woodruff, K. Isolated primate primordial follicles require a rigid physical environment to survive and grow in vitro. *Hum. Reprod.* **2012**, *27*, 1801–1810. [[CrossRef](#)]
11. Sudhakaran, S.; Gualtieri, R.; Barbato, V.; Fiorentino, I.; Braun, S.; Merolla, A.; Talevi, R. Isolated ovarian follicle culture: A promising strategy for fertility preservation. *Curr. Trends. Clin. Embriol.* **2015**, *2*, 177–185.

12. Telfer, E.E. Future developments: In vitro growth (IVG) of human ovarian follicles. *Acta Obs. Gynecol. Scand.* **2019**, *98*, 653–658. [[CrossRef](#)] [[PubMed](#)]
13. Smitz, J.; Dolmans, M.M.; Donnez, J.; Fortune, J.E.; Hovatta, O.; Jewgenow, K.; Picton, H.M.; Plancha, C.; Shea, L.D.; Stouffer, R.L.; et al. Current achievements and future research directions in ovarian tissue culture, in vitro follicle development and transplantation: Implications for fertility preservation. *Hum. Reprod. Update* **2010**, *16*, 395–414. [[CrossRef](#)] [[PubMed](#)]
14. Catapano, G.; Gualtieri, R.; Talevi, R. Transport analysis of bioreactors for the in vitro culture of ovarian tissue. *Curr. Trends. Clin. Embryol.* **2016**, *3*, 54–65. [[CrossRef](#)]
15. Hovatta, O.; Silye, R.; Abir, R.; Krausz, T.; Winston, R.M.L. Extracellular matrix improves survival of both stored and fresh human primordial and primary ovarian follicles in long-term culture. *Hum. Reprod.* **1997**, *12*, 1032–1036. [[CrossRef](#)]
16. Wright, C.S.; Hovatta, O.; Margara, R.; Trew, G.; Winston, R.M.L.; Franks, S.; Hardy, K. Effects of follicle-stimulating hormone and serum substitution on the in-vitro growth of human ovarian follicles. *Hum. Reprod.* **1999**, *14*, 1555–1562. [[CrossRef](#)]
17. Isachenko, V.; Montag, M.; Isachenko, E.; van der Ven, K.; Dorn, C.; Roesing, B.; Braun, F.; Sadek, F.; van der Ven, H. Effective method for in-vitro culture of cryopreserved human ovarian tissue. *Reprod. Biomed. Online* **2006**, *13*, 228–234. [[CrossRef](#)]
18. Liebenthron, J.; Koester, M.; Drengner, C.; Reinsberg, J.; van der Ven, H.; Montag, M. The impact of culture conditions on early follicle recruitment and growth from human ovarian cortex biopsies in vitro. *Fert. Steril.* **2013**, *100*, 483–491. [[CrossRef](#)]
19. Talevi, R.; Sudhakaran, S.; Barbato, V.; Merolla, A.; Braun, S.; Di Nardo, M.; Costanzo, V.; Ferraro, R.; Iannantuoni, N.; Catapano, G.; et al. Is oxygen availability a limiting factor for in vitro folliculogenesis? *PLoS ONE* **2018**, *13*. [[CrossRef](#)]
20. Fraser, I.S.; Baird, D.T.; Cockburn, F. Ovarian venous blood P_{O_2} , P_{CO_2} and pH in women. *J. Reprod. Fert.* **1973**, *33*, 11–17. [[CrossRef](#)]
21. Cargill, W.; Hickam, J.B. The oxygen consumption of the normal and the diseased human kidney. *J. Clin. Investig.* **1949**, *28*, 526–532. [[CrossRef](#)] [[PubMed](#)]
22. Kim, J.; Saidel, G.M.; Cabrera, M.E. Multi-Scale computational model of fuel homeostasis during exercise: Effect of hormonal control. *Ann. Biomed. Eng.* **2006**, *35*, 69–90. [[CrossRef](#)] [[PubMed](#)]
23. Hu, Y.; Betzendahl, I.; Cortvrindt, R.; Smitz, J.; Eichenlaub-Ritter, U. Effects of low O_2 and ageing on spindles and chromosomes in mouse oocytes from pre-antral follicle culture. *Hum. Reprod.* **2001**, *16*, 737–748. [[CrossRef](#)] [[PubMed](#)]
24. Gigli, I.; Cushman, R.A.; Wahl, C.M.; Fortune, J.E. Evidence for a role for anti-Mullerian hormone in the suppression of follicle activation in mouse ovaries and bovine ovarian cortex grafted beneath the chick chorioallantoic membrane. *Mol. Reprod. Dev.* **2005**, *71*, 480–488. [[CrossRef](#)] [[PubMed](#)]
25. Kirkegaard, K.; Hindkjaer, J.J.; Ingersley, H.J. Effect of oxygen concentration on human embryo development evaluated by time-lapse monitoring. *Fert. Steril.* **2013**, *99*, 738–744. [[CrossRef](#)] [[PubMed](#)]
26. Jorssen, E.P.; Langbeen, A.; Fransen, E.; Martinez, E.L.; Leroy, J.L.; Bols, P.E. Monitoring preantral follicle survival and growth in bovine ovarian biopsies by repeated use of neutral red and cultured in vitro under low and high oxygen tension. *Theriogenology* **2014**, *82*, 387–395. [[CrossRef](#)] [[PubMed](#)]
27. Xu, J.; Lawson, M.S.; Yeoman, R.R.; Pau, K.Y.; Barrett, S.L.; Zelinski, M.B.; Stouffer, R.L. Secondary follicle growth and oocyte maturation during encapsulated three-dimensional culture in rhesus monkeys: Effects of gonadotrophins, oxygen and fetuin. *Hum. Reprod.* **2011**, *26*, 1061–1072. [[CrossRef](#)] [[PubMed](#)]
28. Gook, D.A.; Edgar, D.H.; Lewis, K.; Sheedy, J.R.; Gardner, D.K. Impact of oxygen concentration on adult murine pre-antral follicle development in vitro and the corresponding metabolic profile. *Mol. Hum. Reprod.* **2013**. [[CrossRef](#)] [[PubMed](#)]
29. Connolly, J.M.; Kane, M.T.; Quinlan, L.R.; Dockery, P.; Hynes, A.C. Hypoxia limits mouse follicle growth in vitro. *Reprod. Fertil. Dev.* **2015**. [[CrossRef](#)]
30. Zeilmaker, G.H.; Verhamme, C.M. Observations on rat oocyte maturation *in vitro*: Morphology and energy requirements. *Biol. Reprod.* **1974**, *11*, 145–152. [[CrossRef](#)]
31. Van Blerkom, J. Epigenetic influences on oocyte developmental competence: Perifollicular vascularity and intrafollicular oxygen. *J. Assist. Reprod. Genet.* **1998**, *15*, 226–234. [[CrossRef](#)] [[PubMed](#)]

32. Morimoto, Y.; Oku, Y.; Sonoda, M.; Haruki, A.; Ito, K.; Hashimoto, S.; Fukuda, A. High oxygen atmosphere improves human follicle development in organ cultures of ovarian cortical tissues in vitro. *Hum. Reprod.* **2007**, *22*, 3170–3177. [CrossRef] [PubMed]
33. Hovatta, O.; Wright, C.; Krausz, T.; Hardy, K.; Winston, R.M.L. Human primordial, primary and secondary ovarian follicles in long-term culture: Effect of partial isolation. *Hum. Reprod.* **1999**, *14*, 2519–2524.
34. Bird, R.B.; Stewart, W.E.; Lightfoot, E.N. *Transport Phenomena*, 2nd ed.; J. Wiley & Sons: New York, NY, USA, 2002; pp. 303–305, 543–581.
35. Dardik, A.; Chen, L.; Frattini, J.; Asada, H.; Aziz, F.; Kudo, F.A.; Sumpio, B.E. Differential effects of orbital and laminar shear stress on endothelial cells. *J. Vasc. Surg.* **2005**, *41*, 869–880. [CrossRef] [PubMed]
36. Understanding Effects of Viscosity in the BioFlux System. Available online: <https://support.fluxionbio.com/hc/en-us/articles/203649638-Viscosity-Understanding-effects-of-viscosity-in-the-BioFlux-system> (accessed on 29 May 2019).
37. Available online: <https://www.thermofisher.com/order/catalog/product/140620> (accessed on 16 October 2018).
38. Doig, S.D.; Pickering, S.C.R.; Lye, G.J.; Baganz, F. Modelling surface aeration rates in shaken microtitre plates using dimensionless groups. *Chem. Eng. Sci.* **2005**, *60*, 2741–2750. [CrossRef]
39. Kloeckner, W.; Buechs, J. Advances in shaking technologies. *Trends Biotechnol.* **2012**, *30*, 307–313. [CrossRef] [PubMed]
40. Cussler, E.L. *Diffusion: Mass Transfer in Fluid Systems*, 3rd ed.; Cambridge Univ Press: Cambridge, UK, 1984; p. 254.
41. Gosden, R.G.; Byatt-Smith, J.G. Oxygen concentration gradient across the ovarian follicular epithelium: Model, predictions and implications. *Hum. Reprod.* **1986**, *1*, 65–68. [CrossRef] [PubMed]
42. Clark, A.R.; Stokes, Y.M.; Lane, M.; Thompson, J.G. Mathematical modelling of oxygen concentration in bovine and murine cumulus-oocyte complexes. *Reproduction* **2006**, *131*, 999–1006. [CrossRef]
43. Redding, G.P.; Bronlund, J.E.; Hart, A.L. Mathematical modelling of oxygen transport-limited follicle growth. *Reproduction* **2007**, *133*, 1095–1106. [CrossRef]
44. Clark, A.R.; Stokes, Y.M. Follicle Structure influences the availability of oxygen to the oocyte in antral follicles. *Comput. Math. Methods Med.* **2011**. [CrossRef]
45. Schmidt, K.L.T.; Byskov, A.G.; Nyboe Anderson, A.; Mueller, J.; Yding Anderson, C. Density and distribution of primordial follicles in single pieces of cortex from 21 patients and in individual pieces of cortex from three entire human ovaries. *Hum. Reprod.* **2003**, *18*, 1158–1164. [CrossRef]
46. Fogler, H.S. *Elements of Chemical Reaction Engineering*, 4th ed.; Prentice Hall: Westford, MA, USA, 2006; pp. 813–867.



© 2019 by the authors. Licensee MDPI, Basel, Switzerland. This article is an open access article distributed under the terms and conditions of the Creative Commons Attribution (CC BY) license (<http://creativecommons.org/licenses/by/4.0/>).